

Estimation of 3D density distribution of chromites deposit using gravity data

A. Nejadi Kalateh*, A. Roshandel kahoo

Faculty of Mining, Petroleum and Geophysics, Shahrood University of Technology; Shahrood, Iran

Received 17 March 2013; received in revised form 11 July 2013; accepted 24 September 2013

*Corresponding author: nejati@shahroodut.ac.ir (A. Nejadi Kalateh)

Abstract

Surface gravity data is inverted to recover subsurface 3D density distribution with two strategies. In the first strategy, we assumed wide density model bound to invert gravity data, and in the second strategy we carried out the inversion procedure by band limited density. We discretized the earth model into rectangular cells of constant and unidentified density. The number of cells was often greater than the number of observation points. Thus we have an underdetermined inverse problem. The densities were estimated by minimizing a cost function subject to fitting the observed data. The synthetic results show that the recovered model from the first strategy is characterized by broad density distribution around the true model, but the recovered model from the second strategy is closer to true models. To estimate the subsurface density distribution, we carried out inversion of gravity data taken over chromite deposit located at southern part of Iran. The recovered model obtained from the second strategy has appropriate agreement with previous studies.

Keywords: *Density distribution, Positivity constrain, Chromites deposit, Inversion, Gravity data.*

1. Introduction

Potential field data have been widely used in investigations of oil and gas explorations [10], mineral explorations [13] and in engineering studies [5, 16]. The inversion is the most essential step in the quantitative interpretation of potential field data. This step of interpretation of potential field data suffers from the non-unique determination of the source parameters [2]. In other words, the potential field data is acquired on the surface of the earth; there are many equivalent 3D density distributions below the surface that will reproduce the same field data.

Previous papers tried to overcome the inherent non-uniqueness in potential field inverse problems. Some researchers suggested the density variation and attempted to invert the unknown geometrical parameters [4, 11, 14]. Another group of researchers introduced more qualitative prior information. Last and Kubik (1983) minimized the total volume of the source of anomaly and Guillen and Menichetti (1984) used the moment

of inertia of causative body. Barbosa and Silva (1994) introduced the method based on compact gravity inversion technique to allow compactness along the several axis using Tikhonov's regularization method.

In this paper, the model objective function is minimized based on a priori information via positivity density constraints. Firstly, the earth model is divided into rectangular prism with constant and unknown density. The unknown densities are determined by minimizing a model objective function. Positivity density constrain are used to overcome the non-uniqueness problem. The algorithm is tested on both synthetic and field examples.

2. Methodology

The vertical attraction of gravity, g , in Cartesian coordinates for a 3D model such as Figure 1 can be obtained as Equation 1.

$$g_{x,y,z} = -\gamma \int_{z'} \int_{y'} \int_{x'} \rho \frac{z-z'}{r^3} dx' dy' dz' \quad (1)$$

where, ρ is the density distribution, γ is the Newton's gravitational constant, and r can be computed as Equation 2.

$$r = \sqrt{(x-x')^2 + (y-y')^2 + (z-z')^2} \quad (2)$$

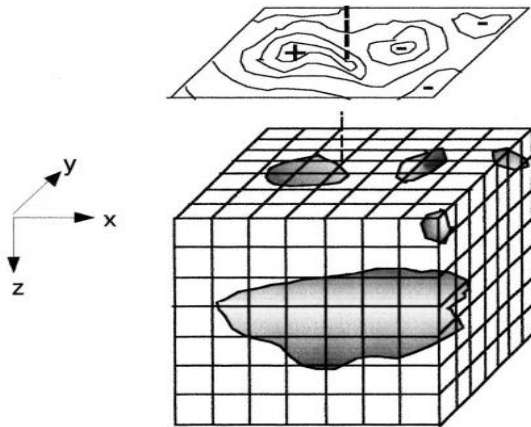


Figure 1. A three-dimensional body with density distribution. Usually, the region to be investigated is subdivided into a set of homogeneities [1].

It is required to discretize the problem for obtaining a numerical solution to the inverse problem of gravity field data. The forward modeling of gravity data defined as Equation 1 can be rewritten as the following matrix equation by dividing the source region into the 3D prism [15].

$$g = G\rho \quad (3)$$

where, G is the kernel matrix which has elements that compute at i th data point of a unit density in j th prism as Equation 4.

$$G_{ij} = -\gamma \int_{z'_j} \int_{y'_j} \int_{x'_j} \frac{z_i - z'_j}{r^3} dx' dy' dz' \quad (4)$$

The data misfit function is given by Equation 5.

$$\phi_g = \left\| W_g (g - g^{obs}) \right\|_2^2 \quad (5)$$

Where, $g^{obs} = [g_{z1}, \dots, g_{zN}]^T$ is the field data vector, g is the predicted data, $W_g = \text{diag} [1/\sigma_1, \dots, 1/\sigma_N]$ and σ_i is the

standard deviation error related with the i th data point.

The model objective function is given by Equation 6.

$$\begin{aligned} \phi_m \rho &= \alpha_s \int_V w_z [\rho - \rho_0]^2 dv \\ &+ \alpha_x \int_V w_x \left\{ \frac{\partial w_z [\rho - \rho_0]}{\partial x} \right\}^2 dv \\ &+ \alpha_y \int_V w_y \left\{ \frac{\partial w_z [\rho - \rho_0]}{\partial y} \right\}^2 dv \\ &+ \alpha_z \int_V w_z \left\{ \frac{\partial w_z [\rho - \rho_0]}{\partial z} \right\}^2 dv \\ &= \left\| W_\rho (\rho - \rho_0) \right\|^2 \end{aligned} \quad (6)$$

where, V is the volume of the causative body, w_x , w_y and w_z are spatially dependent weighting function while α_s , α_x , α_y and α_z are coefficients that defined the relative importance of each components in objective function. w_z is the depth weighting function and ρ_0 is the reference model and W_ρ is the total weight of model parameters [7]. w_z is defined by Equation 7.

$$w_z = \frac{1}{(z - z_0)^{\beta/2}} \quad (7)$$

In Equation 7, β is usually equal to 2.0 [8] and z_0 depends upon the cell size of the model discretization. The reference model ρ_0 can be obtained from previous studies or it can be considered as the zero models. The function w_s controlled the relative similarity of the inverted model to ρ_0 at any position. The weighting functions w_x , w_y and w_z can be used to enhance or attenuate structures in various regions in the model domain [8]. The inverse problem is solved by finding a model ρ that minimizes $\phi_m \rho$ and misfit data function ϕ_g simultaneously. The

inversion process can be done by subspace minimization method [7].

Let $\delta\rho$ denote the perturbation of model parameter. It can be represented as Equation 8.

$$\delta\rho^n = V\alpha \tag{8}$$

where, the vector V are generated mainly from the gradient of data and model objective function [12] and α is the coefficient obtained from Equation 9.

$$L\alpha = l,$$

$$L = V^T F^T G^T W_g^T W_g G + \lambda W_\rho^T W_\rho FV$$

$$l = -V^T F^T G^T W_g^T W_g g^n - g^{obs}$$

$$-\lambda V^T F^T G^T W_\rho^T W_\rho \rho^n - \rho_0$$
(9)

Where, F is the Jacobean matrix of model parameters, λ is the Lagrangian multipliers and n is the number of iterations. The final model parameters computed as Equation 10.

$$\rho = \rho_0 + \delta\rho^n \tag{10}$$

3. Synthetic example

As a first example the gravity data shown in Figure 2 is inverted. It is produced by two rectangle block model at depth 25m, 50m and 150m, 250m on side respectively. Density contrast of two rectangle block set to 1.0 g/cm^2 . The data is free noise and data

grid spacing is 50m. A model consisting of 1600 cells of 25 m in each depth level is used and the model extends from 0 to 500m ($40*40*20$).

We invert the gravity data by considering a wide density model bound between -3.0 g/cm^3 and 3.0 g/cm^3 for studying

effect of density constrains to recover synthetic model. The model objective function defined in Equation 6 is minimized in which $\alpha_s = 0.0001$

and $\alpha_x = \alpha_y = \alpha_z = 1.0$. 3-D weighting

functions are set to 1.0 because, there is no preferred density distribution in each direction of synthetic model and the depth weighting parameters are considered with $\beta = 2.0$ in Equation 7. The recovered model data is shown in Figure 3 [8].

The recovered model shown in Figure (3) is characterized by broad density distribution around the true model (shown as white rectangle blocks).

The range of inverted density model is obtained between -0.18 to 0.99 g/cm^3 . Root mean square error between model gravity data and predicted data is 0.01 mGal .

Next we inverted same data with positivity density constraint. Maximum density contrast was equal to 1.0 g/cm^3 . It's useful when a reliable estimate of maximum density contrast is available. Imposition of such a bound can often improve density distribution in recovered model. The result is shown in Figure (4).

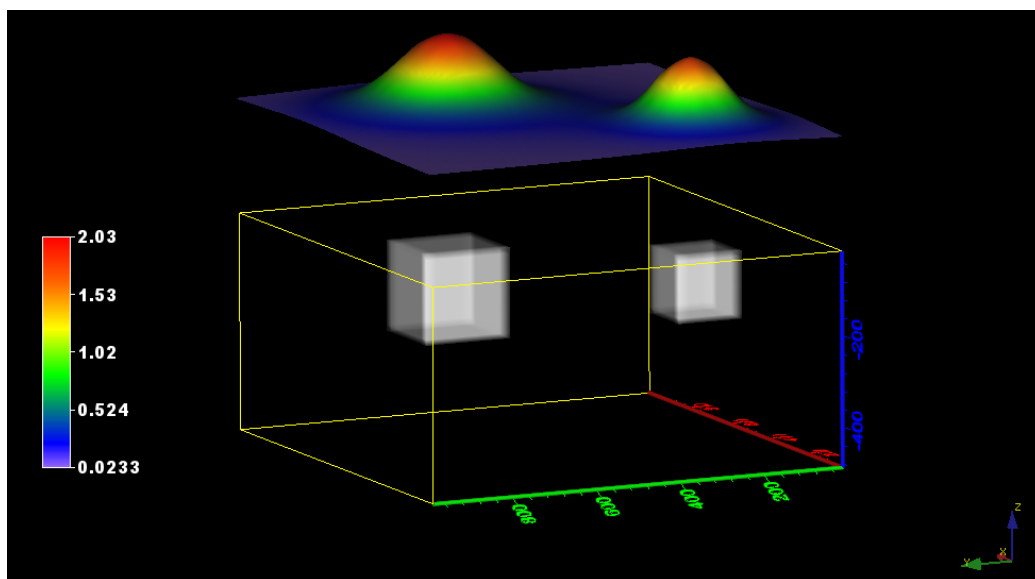


Figure 2. Gravity data was produced by two rectangle model having density of 1.0 g/cm^2 and uniform background. The color scale indicated the gravity data in mGal.

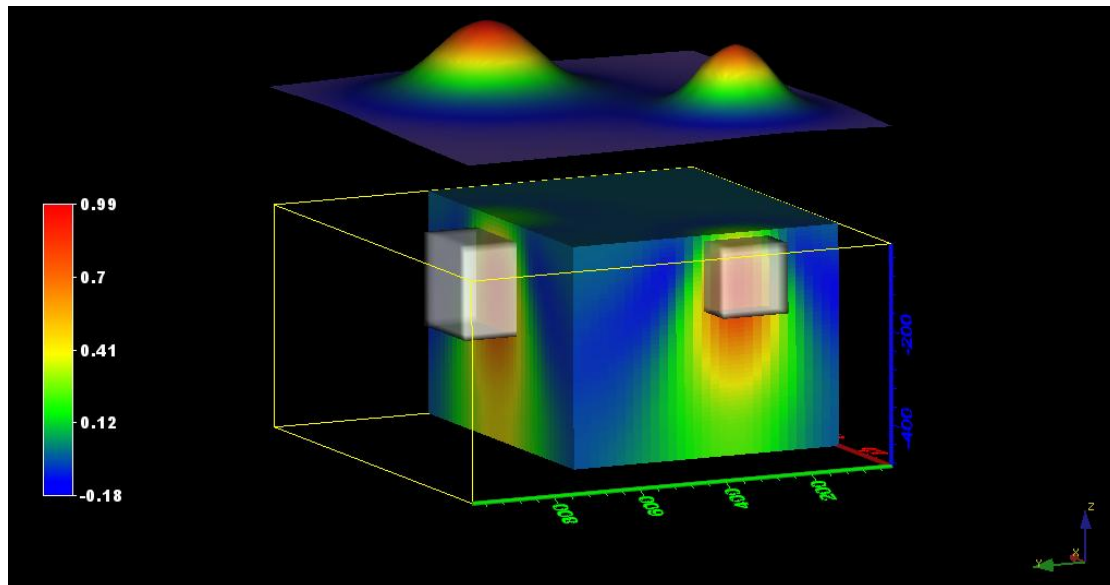


Figure 3. Recovered density model of free noise gravity data. The color scale indicates the density distribution in g/cm^3 . Synthetic models are shown with white rectangle blocks.

Considering density constraint, synthetic model has been recovered well and density distribution concentrates at the location of true model. Root mean square error between synthetic gravity data and predicted data is 0.01 mGal . The maximum density value is slightly less than 1.0 g/cm^3 , which is in fact very close to the true maximum density value in this case. Overall, we have a reasonably recovered model that delineates the essential structure of the true model.

Figure 5 shows the same data contaminated with 2% independent Gaussian white noise. Recovered density distributions are characterized by broad tails at depth like Figure 3 and focus on the top of synthetic model. Root mean square error between model gravity data and predicted data is 0.069 mGal .

We invert the noisy data with limited band of density between 0.0 and 1.0 g/cm^3 . Root mean square error between model gravity data and predicted data is 0.063 mGal . The Result is shown in Figure 6. The recovered anomalies also appear at the depth that corresponds well with the true depth of the rectangle model. Results shows that the density constrains are effective in placing the recovered anomaly at depth of the true causative body.

4. Real data

As a final example, field data taken over a chromite deposit located at southern part of Iran is inverted. The host rocks of deposit are Serpentine.

The chromite veins may extend into fractured Serpentine rocks. The gravity data are acquired in the study area (shown in Figure 7) with 10m spacing along 8 lines in the north-east direction and spaced 10 m apart. Our study of the data set has focused on a part of data shown in Figure 8. Y axis indicates north direction. In study area experimental methods are used to determine the mean density. The average density of host rocks is 2.79 g/cm^3 and the average density in a relatively pure sample of chromite is measured 4.0 g/cm^3 approximately. The depth model parameterization is extended to 40 m. Root mean square error between real gravity data and predicted data is 0.015 mGal .

According to Figure 8, maximum density distribution is concentrated at depth 20 m approximately. Nejati et. al. (2005) showed that most volume of chromite mineralization in prospected area located at the depth of 20 m by 3D compact inversion of gravity data [9].

5. Conclusions

In this paper, 3D density distribution was obtained by Li and Oldenburg (1998) method with two strategies. In the first strategy, wide density model bound was assumed to invert synthetic and real gravity data. The results show that the recovered model is characterized by broad density distribution around the true model. In the second strategy, the inversion procedure was carried out

by band limited density. When the reliable estimation of maximum density contrast was available from geological and geophysical prior investigation, the results of second strategy were closer to true models. We carried out the inversion

of gravity data taken over chromite deposit located at south part of Iran to estimate subsurface density distribution. The recovered model obtained from second strategy has appropriate agreement with previous studies.

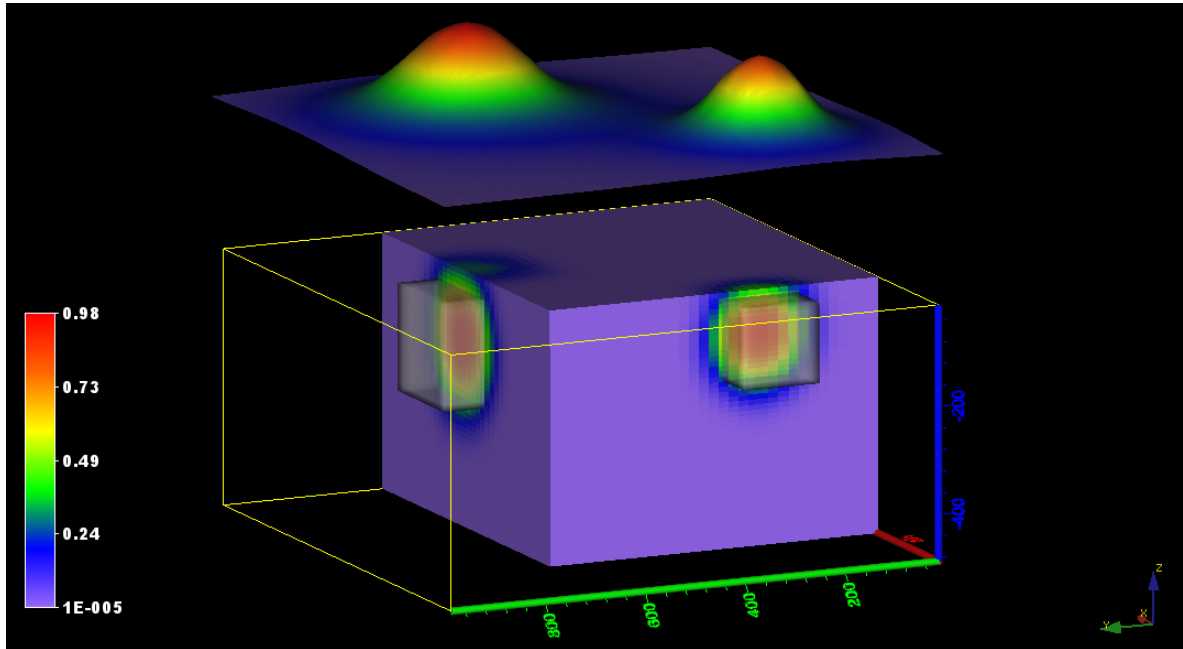


Figure 4. Recovered density model of free noise gravity data with density constrain between 0.0 to 1.0 g / cm^3 . The color scale indicates the density distribution in g / cm^3 . Synthetic models are shown with white rectangle blocks.

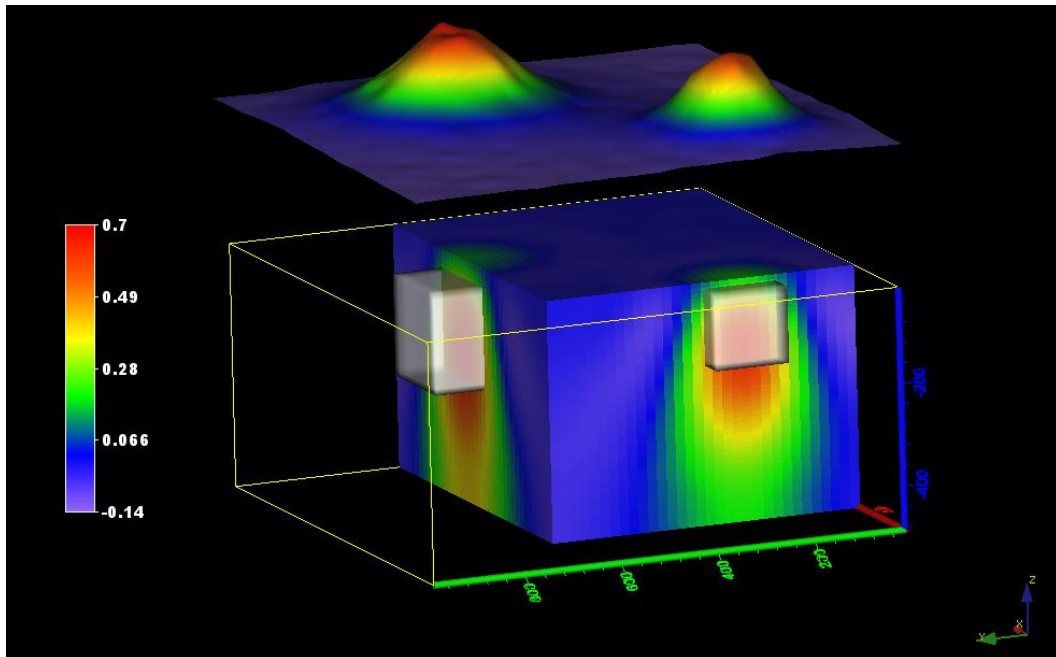


Figure 5. Data contaminated with 2% independent Gaussian white noise. The color scale indicates the density distribution in g / cm^3 . Synthetic models are shown with white rectangle blocks.

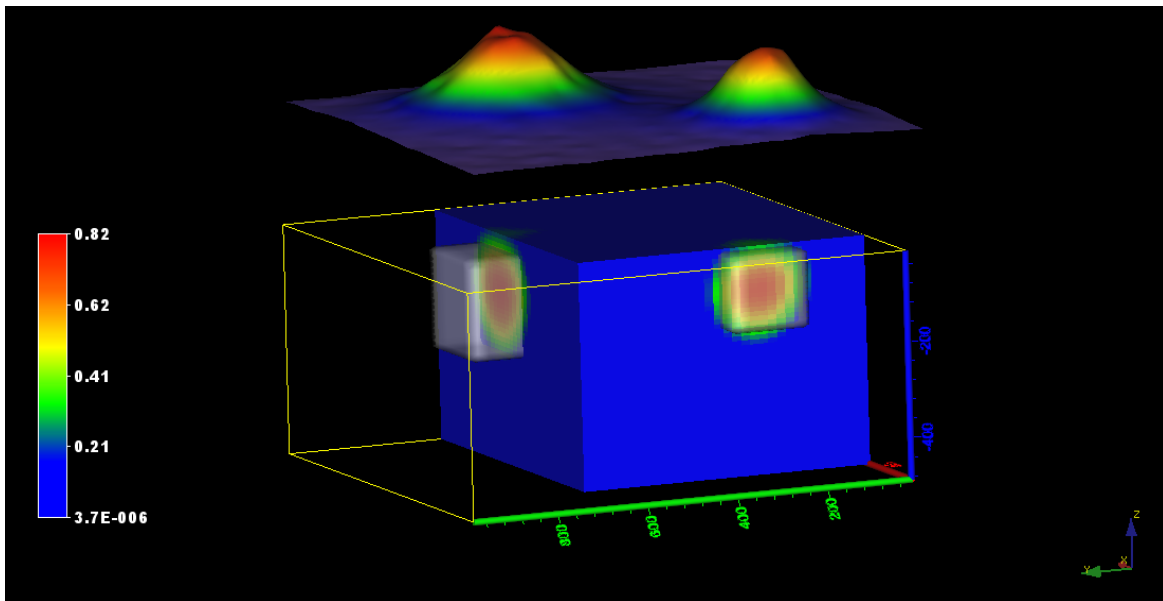


Figure 6. Noisy data and inverted density distribution. The color scale indicates the density distribution in g / cm^3 . Synthetic models are shown with white rectangle blocks.

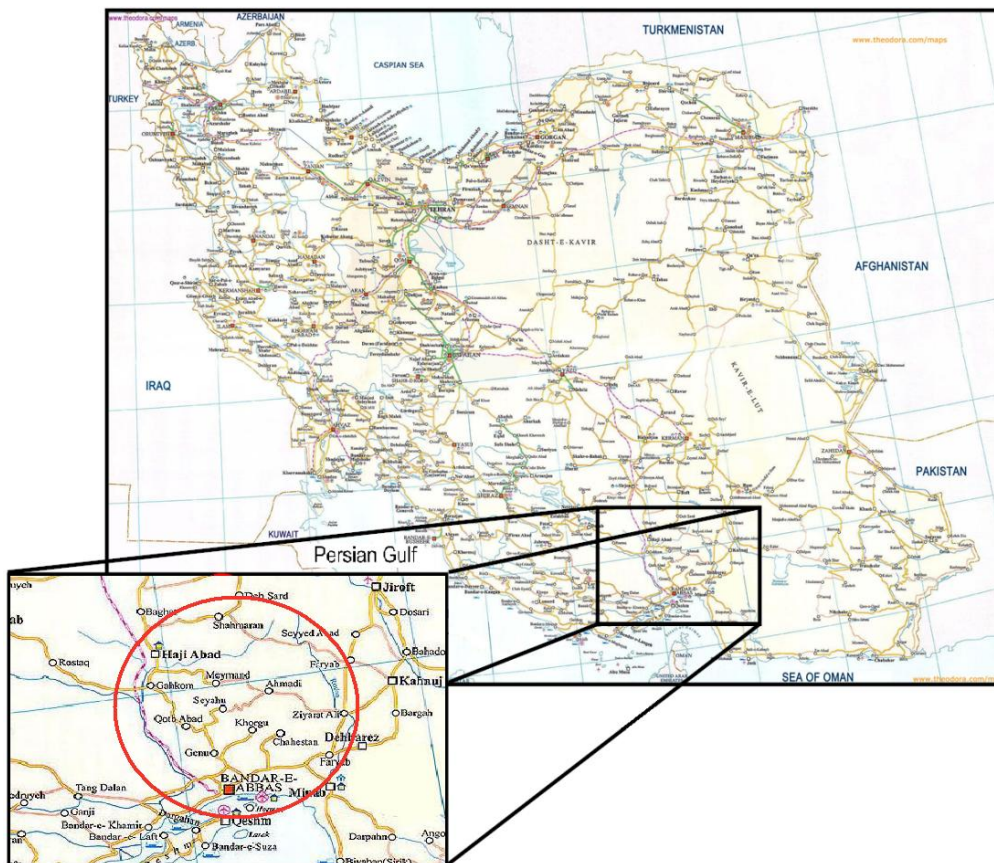
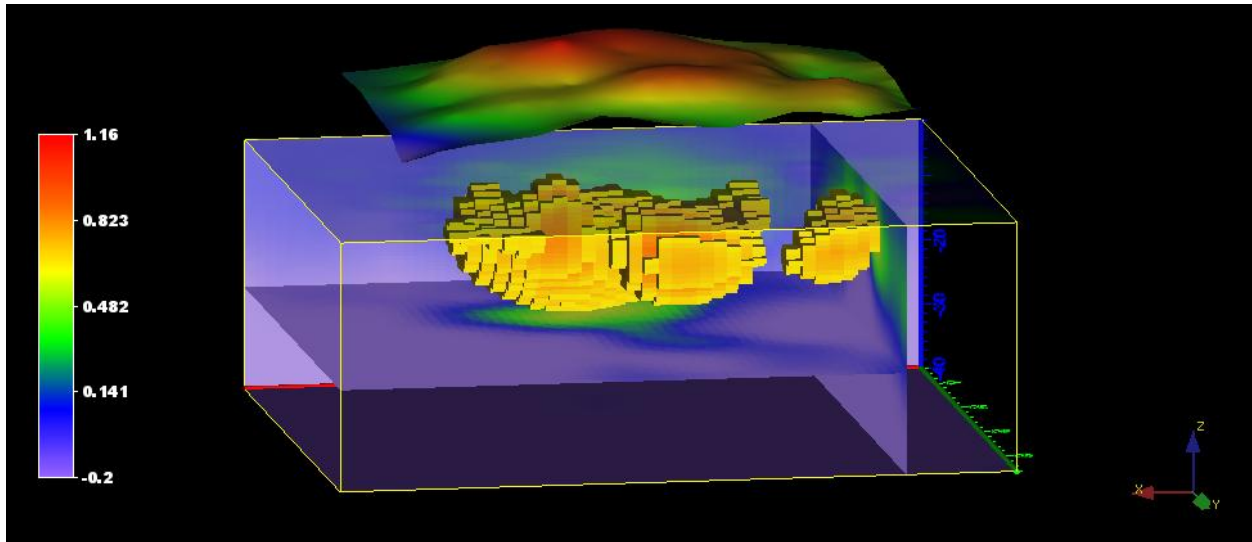
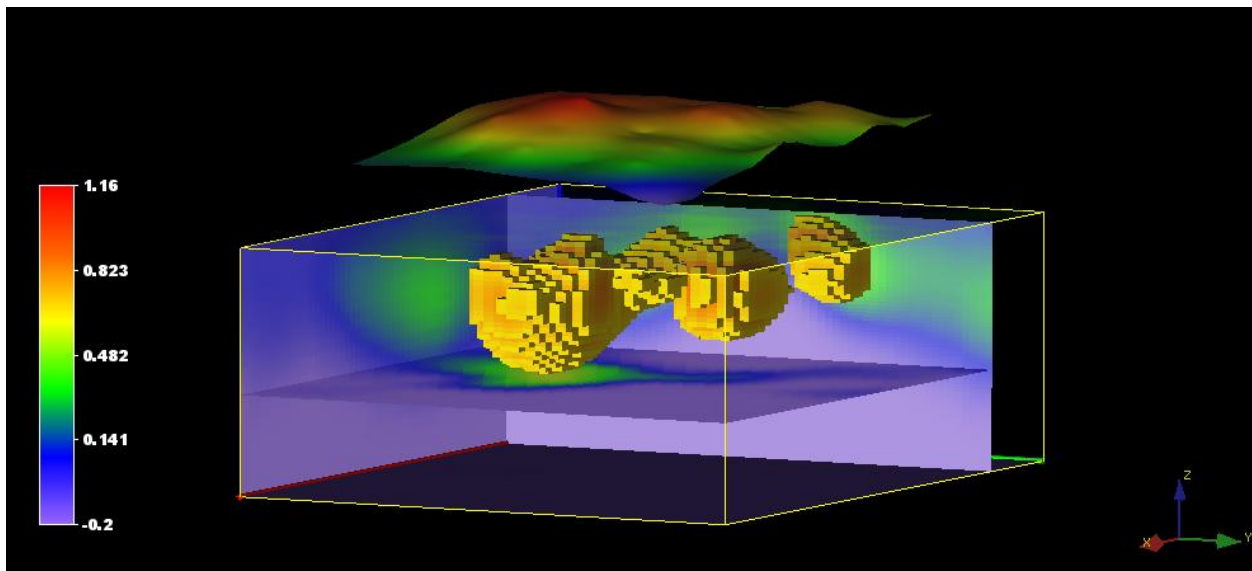


Figure 7. Location map of study area



(a)



(b)

Figure 8. Real data and inverted density distribution. The color scale indicates the density distribution in g / cm^3 . Y- axis is north direction. a) Y- axis out of the page and b) Y- axis in the right direction.

References

- [1]. Barbosa, V. C. F. and Silva, J. B. C. (1994). Generalized compact gravity inversion. *Geophysics*. 59(1): 57–68.
- [2]. Fedi, M. and Rapolla, A. (1999). 3-D inversion of gravity and magnetic data with depth resolution. *Geophysics*. 64(2): 452-460.
- [3]. Guillen, A. and Menichetti, V. (1984). Gravity and magnetic inversion with minimization of a specific functional. *Geophysics* 49(8): 1354-1360.
- [4]. Guspi, F. (1992). Three-dimensional Fourier gravity inversion with arbitrary density contrast. *Geophysics*. 57(1): 131–135.
- [5]. Hinze, W.J. (1990). The role of gravity and magnetic methods in engineering and environmental studies. In: Stanley H.W. (Ed.). *Geotechnical and Environmental geophysics*. Society of exploration geophysics (SEG), 398 p.
- [6]. Last, B. J. and Kubik, K. (1983). Compact gravity inversion. *Geophysics*. 48(6): 713-721.

- [7]. Li, Y. and Oldenburg, D. W. (1996). 3-D inversion of magnetic data. *Geophysics*. 61(2): 394–408.
- [8]. Li, Y. and Oldenburg, D. W. (1998). 3-D inversion of gravity data. *Geophysics*. 63(1): 109–119.
- [9]. Nejati Kalateh, A. Ardestani, V.E.Z. Zomorodian. H. and Shahin, E. (2005). 3-D Modeling of Gravity Data Using Compact Inversion (In Persian). *Journal of Geosciences*. 14: 18-29.
- [10]. Nejati Kalateh, A. Mirzaei, M. Gouya, N. and Shahin, E. (2010a). Non-linear inversion of magnetic data using gradient subspace method (In Persian). *Journal of Geosciences*. 19: 165-172.
- [11]. Nejati Kalateh, A. Siahkoohi, H.R. Mirzaei, M. and Gouya, N. (2010b). Inverse Modeling of Magnetic Data Using Subspace Method (In Persian): *Iranian journal of Geophysics*. 4(2): 13-31.
- [12]. Oldenburg, D. W. and Li, Y. (1994). Subspace linear inversion methods. *Inverse Problems*. 10: 915-935.
- [13]. Paterson, N. R. and Reeves, C. V. (1985). Applications of gravity and magnetic surveys: The state-of-the-art in 1985. *Geophysics*. 50 (12): 2558–2594.
- [14]. Pedersen, L. B. (1977). Interpretation of potential field data: A generalized inverse approach. *Geophys. Prosp.* 25(2) 199–230.
- [15]. Plouff, D. (1976). Gravity and magnetic-fields of polygonal prisms and application to magnetic terrain corrections . *Geophysics*. 41(4): 727-741.
- [16]. Ward, S. H. (1990). Geotechnical and environmental geophysics (Investigations in Geophysics), SEG. 300 pp.